

Enhanced optical coupling and Raman scattering via microscopic interface engineering

Jonathan V. Thompson,¹ Brett H. Hokr,¹ Wihan Kim,¹ Charles W. Ballmann,¹ Brian E. Applegate,¹ Javier A. Jo,¹ Alexey Yamilov,² Hui Cao,³ Marlan O. Scully,^{1,4} and Vladislav V. Yakovlev^{1,a)}

¹Texas A&M University, College Station, Texas 77843, USA

²Missouri University of Science & Technology, Rolla, Missouri 65409, USA

³Yale University, New Haven, Connecticut 06520, USA

⁴Baylor University, Waco, Texas 76798, USA

(Received 5 September 2017; accepted 2 November 2017; published online 14 November 2017)

Spontaneous Raman scattering is an extremely powerful tool for the remote detection and identification of various chemical materials. However, when those materials are contained within strongly scattering or turbid media, as is the case in many biological and security related systems, the sensitivity and range of Raman signal generation and detection is severely limited. Here, we demonstrate that through microscopic engineering of the optical interface, the optical coupling of light into a turbid material can be substantially enhanced. This improved coupling facilitates the enhancement of the Raman scattering signal generated by molecules within the medium. In particular, we detect at least two-orders of magnitude more spontaneous Raman scattering from a sample when the pump laser light is focused into a microscopic hole in the surface of the sample. Because this approach enhances both the interaction time and interaction region of the laser light within the material, its use will greatly improve the range and sensitivity of many spectroscopic techniques, including Raman scattering and fluorescence emission detection, inside highly scattering environments. *Published by AIP Publishing.* <https://doi.org/10.1063/1.5003363>

The use of Raman scattering has proven to be a powerful way to detect substances with high chemical specificity. It has been used effectively in a variety of circumstances, ranging from the remote sensing of subsurface water temperatures¹ to material/biomedical imaging^{2–6} and the detection of explosive or harmful substances.^{7–9}

Unfortunately, the signal from spontaneous Raman scattering is weak, requiring the use of expensive and sensitive detectors, as well as long integration times. For this reason, many complementary techniques and methods, built on the fundamental principle of Raman scattering, have been developed to enhance signal and decrease acquisition time. Some of these techniques include stimulated Raman scattering,^{10,11} coherent anti-Stokes Raman scattering,^{8,12} and surface enhanced Raman scattering.¹³ Other methods use integrating cavities^{14,15} to increase the interaction time and region of the laser light within the sample, thereby enhancing signal and sensitivity.

In many instances, the substance or chemical of interest is either contained in or behind a highly scattering material. This imposes a limitation on the effectiveness of both spontaneous Raman scattering as well as the previously mentioned enhancement techniques. For example, the optical detection of a harmful substance, such as anthrax, is more challenging when it is contained inside a scattering envelope.^{16,17} The presence of a scattering material reduces the intensity of light that can actually penetrate to the chemical and generate spectroscopic signals. This limitation is very common in biomedical applications where imaging/detection of structures beneath the surface of skin, bone, or other tissue

would allow for the detection of cancer^{18–20} or other diseases.²¹ One way to overcome this limitation of penetration depth is to use either dielectric bandpass filters²² or an achromatic one-way mirror using spatial coherence²³ as effective one-way mirrors to recycle pump light back into the turbid medium. This forces the light deeper, increasing the penetration depth and Raman scattered signal.

Recently, techniques like optical phase conjugation^{24,25} and wavefront shaping have offered ways to focus light through a scattering material^{26–29} to enhance Raman scattering³⁰ or other³¹ signals. Ultimately, these techniques are also limited by the penetration depth of the light through the material. While the transmission of light through the material can be enhanced via wavefront shaping^{32,33} methods, access to both sides of the material are required. In other words, for a system where only epi detection is allowed, a feedback method like fluorescence^{31,34} or Raman scattering³⁰ must be used, yet these methods require adequate penetration of the pump light to begin with. Therefore, in order to acquire Raman scattering signal from deep inside a turbid medium, there is a need to first enhance the penetration depth and interaction time of the light with the medium. Once this is achieved, techniques like wavefront shaping can work in tandem to further enhance the signal generated by the desired chemicals.^{35,36}

The elastic scattering of light can be used to increase the optical path length, and interaction time, of light with molecules within a material.^{37,38} For instance, using highly scattering materials as the walls of an integrating cavity¹⁵ has led to more sensitive detection of fluorescent markers in fluids.¹⁴ Furthermore, adding small amounts of scattering materials to a transparent fluid has also shown some degree of

^{a)}Electronic mail: yakovlev@bme.tamu.edu

signal enhancement.³⁸ While these techniques were demonstrated for transparent or nearly transparent samples, the working principle is that elastic scattering of light can increase optical path length and interaction time with a substance, thereby enhancing spectroscopic signals. For highly scattering materials, the scattering medium itself can be used to obtain this increased path length. In practice, the main obstacle to the realization of this effect is the short penetration depth of light incident on the surface of turbid media. Because most of the light is scattered near the surface of the material, it is not injected deep enough to realize an increased path length due to multiple scattering events.

Recently, we have shown that the enhanced coupling of light into turbid media can be achieved by microscopic engineering of the geometry of the optical interface.³⁹ In this letter, we extend the previous results to show that when light is more efficiently coupled into a turbid medium, it facilitates a drastic improvement on the sensitivity of spectroscopic detection techniques. While this phenomenon has recently been observed in the form of laser crater enhanced Raman scattering,⁴⁰ here we show, through Raman imaging and high resolution temporal detection, that this phenomenon is due to the improved coupling of light into the medium. When the coupling of laser light into a turbid medium is enhanced, the light becomes trapped by scattering within the material for longer periods of time. This drastically enhances the interaction time of the pump laser with the molecules, thereby enhancing spectroscopic signal. This concept is illustrated in Fig. 1. In particular, here we will show that the enhanced interaction time and penetration distance of the pump light within a turbid medium can yield at least two orders of magnitude enhancement in the spontaneous Raman scattering signal generated by the medium.

These results, namely, the enhanced spectroscopic signal and penetration depth, directly influence remote detection methods, including spatially offset Raman spectroscopy.^{41,42} This technique also makes it possible to sensitively detect small concentrations of chemicals in a material using relatively inexpensive detectors. Furthermore, the combination of this approach with wavefront shaping techniques may yield even greater enhancements and finer control of the signal generated.^{35,36}

Barium sulfate (BaSO_4) powder (Sigma Aldrich, 243353) was packed into a 1 in. lens tube (Thorlabs, SM1L03, 1 cm

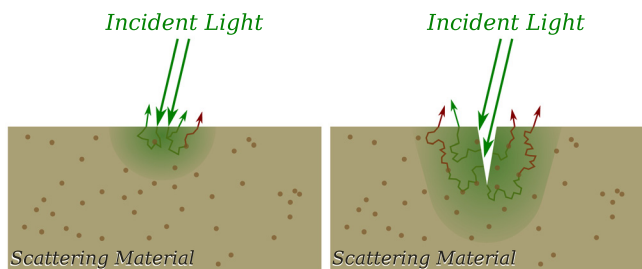


FIG. 1. When light is incident upon a scattering material which contains Raman active particle, the limited penetration depth restricts the interaction of light with the particles (left), and thereby the amount of Raman signal generated. Enhanced coupling of light into a turbid medium is achieved by focusing the light into a microscopic interface engineered in the surface (right). This coupling increases the interaction time and region of light within the material, which directly impacts the amount of generated Raman signal.

thick) to form a highly scattering sample. Barium sulfate was chosen for its high scattering coefficient ($\mu_s = 2083 \text{ mm}^{-1}$), simple Raman spectrum,⁴³ and its ability to be physically packed into a container. In this case, BaSO_4 served as both the scattering medium and the source of Raman scattering, but this method is also applicable to the case where the source of Raman scattering is not the same material as the strongly scattering particles. Once packed, a microscopic hole approximately $300 \mu\text{m}$ deep and $100 \mu\text{m}$ in diameter was engineered into the surface of the sample using laser ablation from 6 ps laser pulses (Attodyne, APL-X, 532 nm) with $35 \mu\text{J}$ of energy per pulse. These pulses were focused onto the sample with a 50 mm lens, and multiple pulses were fired until the ablation reached a saturation point. The cross-section of a characteristic hole was measured using optical coherence tomography³⁹ and is shown in Fig. 2. Laser light was coupled into the packed powder by focusing the laser light into the hole with the same 50 mm lens used to create the hole. Laser light can be uncoupled from the hole by translating the sample in the transverse direction such that the light is incident upon the flat face of the sample and does not enter the hole. While the holes were ablated with laser energies at $35 \mu\text{J}$ per pulse, all measurements (unless noted) were obtained with the laser energy at 150 nJ per pulse.

The spatial profile of the Raman scattered light emitted from the sample in the backward direction was imaged onto a CCD (Mightex CGE-B013-U) with a long pass filter (Semrock LP03-532RS-25) to reject the 532 nm laser light. The measured profiles with and without a hole present are shown on the left in Fig. 3. With equivalent scales, we see the enhancement of the Raman scattering produced near the focus of the laser. We also see the enhancement of Raman light emitted further away from the laser focus. This is more clearly visible when the laser focus is blocked by placing a needle in an intermediate image plane and plotting the image in log scale, as is shown on the right in Fig. 3.

The normalized Raman spectra of the BaSO_4 sample measured for cases with the laser light coupled/uncoupled into the microscopic hole are shown in Fig. 4. These spectra were measured with a fiber-coupled, uncooled spectrometer

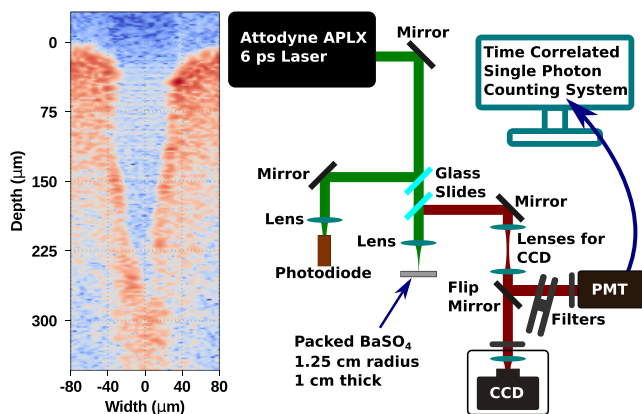


FIG. 2. Cross section (left) of hole ablated in packed BaSO_4 powder as measured by optical coherence tomography. On the right, the experimental setup used to acquire images and the temporal profile of the Raman scattered light is shown. The lenses for the CCD were removed for the temporal measurements (time correlated single photon counting). Raman Spectra were also collected by replacing the CCD with a fiber coupled spectrometer.

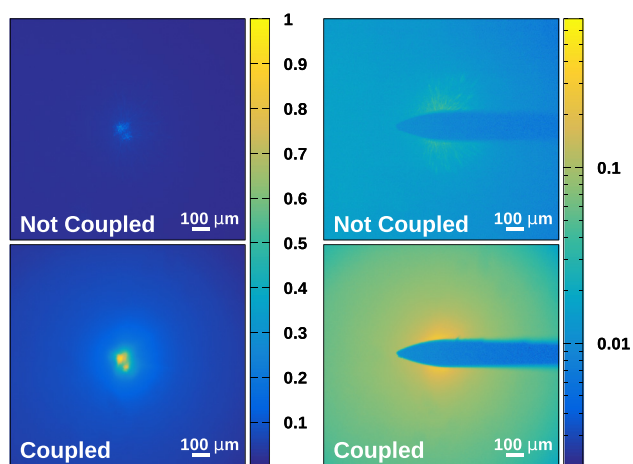


FIG. 3. Images of spontaneous Raman scattering from packed BaSO_4 powder samples. More Raman signal is observed when the pump laser light is coupled (bottom) into the sample through a microscopic hole in the surface. For comparison, the case without a microscopic interface (Not coupled) is also shown (top). A needle was used (right) to block out the focus of the laser, showing that more intense Raman scattered light is observed at distances far away from the laser focus when the pump laser is injected into the microscopic interface. This indicates that the spatial diffusion of the pump light has increased significantly.

(ASEQ, LR1), and show at least two orders of magnitude enhancement of the Raman scattered light from the BaSO_4 powder when the pump laser was more efficiently coupled into the sample.

Time correlated single photon counting (TCSPC)⁴⁴ was employed to measure the time dynamics of the emission of Raman scattered light. As shown in Fig. 2, the Raman light emitted in the backward direction was collected by the focusing lens, and directed through neutral density filters and a long-pass (Semrock LP03-532RS-25) filter into a photomultiplier tube (Hamamatsu R3809U-50). The long-pass filter was used to reject the elastically scattered light, and pass the Raman scattered signal. The neutral density filters were used to control the intensity of the Raman signal on the photomultiplier tube. The electronic signal from the photomultiplier tube was amplified (Hamamatsu C5594-12) and used as the signal for a TCSPC card (SPC-150, Becker-Hickl). A pulse from the laser was also used as a temporal reference. By counting the arrival time of many photons, a statistical

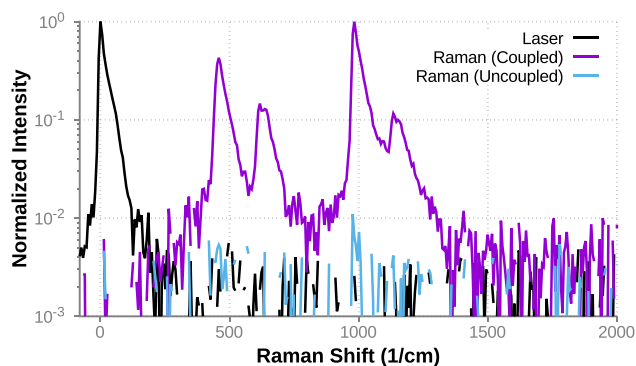


FIG. 4. Normalized spectral intensity of Raman scattering from a BaSO_4 sample with the pump laser coupled (violet) vs uncoupled (blue) into the sample through a microscopic hole. The laser spectrum is given for reference (black). Note that the spectrum for the uncoupled case was normalized by the peak Raman intensity (at 985 cm^{-1}) of the coupled case.

representation of the Raman scattered light with resolution of less than 50 ps (Ref. 44) was accumulated. One benefit of using this method is the extremely large dynamic range achievable by simply counting more photons. More than adequate signal to noise was achieved for Raman generated light by integrating photons at a rate of 10 kHz for approximately 60 min, with the laser running at a repetition rate of 1 MHz with 150 nJ per pulse.

From the temporal picture acquired of the Raman scattered light, shown in Fig. 5, we see a vast increase in the interaction time of the laser with the sample when the laser is focused into the hole in the surface of the sample. More specifically, more than 25 ns after the laser pulse has arrived, there is still a significant amount of Raman light being emitted from the sample. This is an enhancement of over two orders of magnitude more light emitted at this point in time when compared to the case of a sample without a hole.

A better understanding of the substantial amount of Raman scattered light generated by the coupled sample is gained from Fig. 6. This image was acquired using a cellular phone camera (Huawei, Nexus 6P) with laser safety glasses (Thorlabs, LG12) used to filter out the elastically scattered pump light. In this figure, the pump laser was set to approximately 35 μJ per pulse. From this image, we see that the Raman scattering from the coupled sample was brightly visible to the unaided, human eye. We also see that a large portion of the sample surface is emitting Raman scattered light (the sample diameter is 2.5 cm). Even with the laser energy turned down to 150 nJ per pulse, the Raman scattering was clearly visible by eye, and could be used as an indicator of the quality of the laser coupling alignment.

In addition to the large spectroscopic enhancements provided by microscopic interface engineering, samples can be conveniently transplanted to light sources other than the laser used to create the interface. To demonstrate this, a hole was drilled into a packed powder sample using the picosecond laser as previously explained. This sample was removed from the ablation setup, and placed into the beam of a continuous wave diode pumped solid state laser (532 nm) with 2.5 mW of optical power at the sample. The laser beam was

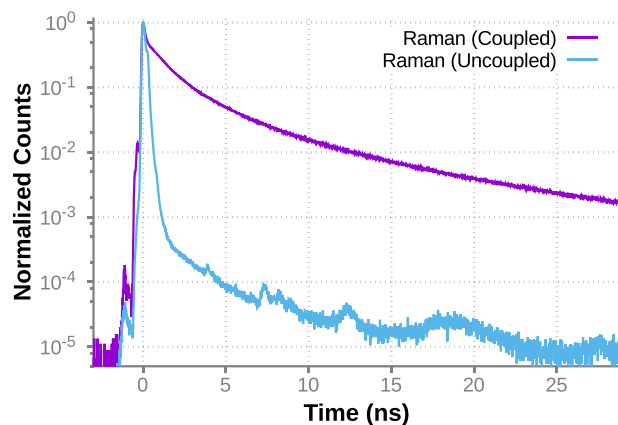


FIG. 5. Normalized intensity of Raman scattering signal detected as a function of time for samples with (violet) and without (blue) a microscopic hole. As the average interaction time of the pump light inside the sample increases, the number of inelastically scattered (i.e., Raman) photons is greatly enhanced.

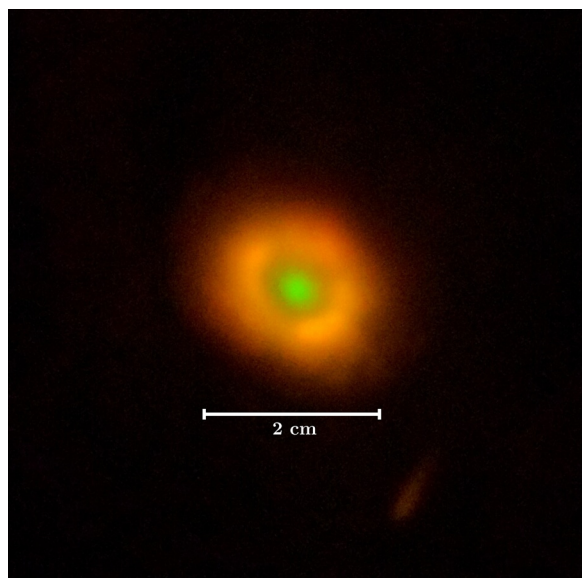


FIG. 6. Image of Raman scattering from a BaSO_4 sample acquired using a cell phone camera and laser safety glasses (Thorlabs, LG12) to filter out the scattered pump light. This image illustrates the substantial enhancement achieved by this method, as the Raman scattering signal is clearly visible by the unaided eye.

focused into the hole using a 50 mm lens. Alignment/coupling of the laser into the microscopic structure was achieved here by monitoring the enhancement of the diffusion radius and transmission³⁹ of the elastically scattered light in the sample as the sample was translated with respect to the beam. The surface of the sample was imaged in the backward direction using an uncooled CCD (Mightex CGE-B013-U), and the images were acquired with 15 ms integration times. These images are shown in Fig. 7, and again, nearly two orders of magnitude ($91\times$) more Raman light was detected near the focus of the laser. Note that Fig. 7 is plotted in log scale in order to show the additional features visible from distances well over $300\ \mu\text{m}$ away from the microscopic structure and laser focus. It is also important to note that here the uncoupled image was obtained by translating the sample in the transverse direction, such that the laser was focused onto the flat sample surface, and no longer coupled. Even though the light is not coupled into the hole, Fig. 7 (left) shows a localized spot of Raman scattered light emitted from the hole (about $400\ \mu\text{m}$ to the right of the laser focus). This

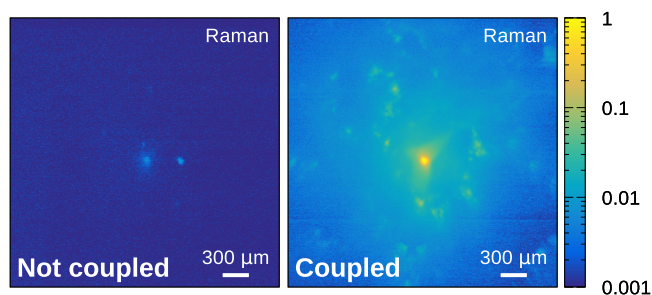


FIG. 7. Image of Raman scattering from a BaSO_4 sample comparing cases when the pump laser was coupled (right) vs uncoupled (left) into the microscopic hole in the surface of the sample. These images were acquired in 15 ms using an uncooled CCD, and about 2.5 mW of optical pump power (cw). Nearly two orders of magnitude more Raman scattered light was detected near the focal region when the light was coupled into the hole.

suggests that this type of structure may be used to both couple light into and out of the turbid medium.

In conclusion, we have demonstrated enhanced optical coupling and Raman scattering of light in a turbid medium by focusing the pump laser light into an engineered microscopic optical interface. In particular, we have observed two orders of magnitude enhancements in the measured Raman scattering signal from a barium sulfate (BaSO_4) sample. This enhancement comes from the increased coupling, penetration depth, and interaction time of the laser with the sample, and is a direct result of utilizing the large elastic scattering coefficient to more effectively contain light inside the turbid medium.

While this method is not entirely non-invasive, the size of the hole ablated in the surface of the material is very small compared to the size of the sample itself, and is at least two to five times smaller than typical hypodermic needles (Ted Pella, Inc.). Furthermore, because it is a geometry related effect, narrower and deeper holes should further improve this coupling of light into the medium, yielding even larger interaction times and Raman signal. Because this technique increases both the interaction time and the spatial interaction region of the pump laser within a material, it is an excellent way to increase the signal from low concentrations of particles distributed throughout the medium. In some instances, it may even facilitate Raman-based detection of chemicals using the unaided, human eye. Lastly, this technique may be an ideal method to improve the sensitivity of remote sensing applications because both sample preparation (hole drilling) and interrogation can be achieved remotely.

This research was supported in part by the National Science Foundation (CBET Award No. 1250363, DBI Award No. 1455671, ECCS Award No. 1509268, and ECCS Award No. 1509361), the Robert A. Welch Foundation (Grant No. A-1261), the Office of Naval Research (Grant Nos. N00014-16-1-3054 and N00014-13-1-0649), and the U.S. Department of Defense (Grant No. FA9550-15-1-0517). J.V.T. was supported by the Herman F. Heep and Minnie Belle Heep Texas A&M University Endowed Fund held/administered by the Texas A&M Foundation. B.H.H. acknowledges a graduate fellowship from the Department of Defense Science, Mathematics and Research for Transformation (SMART) fellowship program.

¹D. A. Leonard, B. Caputo, and F. E. Hoge, *Appl. Opt.* **18**, 1732 (1979).

²C. H. Camp, Jr. and M. T. Cicerone, *Nat. Photonics* **9**, 295 (2015).

³C. Krafft, I. W. Schie, T. Meyer, M. Schmitt, and J. Popp, *Chem. Soc. Rev.* **45**, 1819 (2016).

⁴A. J. Traverso, J. V. Thompson, Z. A. Steelman, Z. Meng, M. O. Scully, and V. V. Yakovlev, *Anal. Chem.* **87**, 7519 (2015).

⁵B. H. Hokr, J. V. Thompson, J. N. Bixler, D. T. Nodurft, G. D. Noojin, B. Redding, R. J. Thomas, H. Cao, B. A. Rockwell, M. O. Scully, and V. V. Yakovlev, *Sci. Rep.* **7**, 44572 (2017).

⁶J. V. Thompson, J. N. Bixler, B. H. Hokr, G. D. Noojin, M. O. Scully, and V. V. Yakovlev, *Opt. Lett.* **42**, 2169 (2017).

⁷S. Ben-Jaber, W. J. Peveler, R. Quesada-Cabrera, E. Cortés, C. Sotelo-Vazquez, N. Abdul-Karim, S. A. Maier, and I. P. Parkin, *Nat. Commun.* **7**, 12189 (2016).

⁸M. O. Scully, G. W. Kattawar, R. P. Lucht, T. Opatrny, H. Pilloff, A. Rebane, A. V. Sokolov, and M. S. Zubairy, *Proc. Natl. Acad. Sci. U.S.A.* **99**, 10994 (2002).

- ⁹S. Wallin, A. Pettersson, H. Östmark, and A. Hobro, *Anal. Bioanal. Chem.* **395**, 259 (2009).
- ¹⁰R. W. Boyd, *Nonlinear Optics*, 3rd ed. (Academic Press, Burlington, MA, 2008).
- ¹¹B. H. Hokr, J. N. Bixler, M. T. Cone, J. D. Mason, H. T. Beier, G. D. Noojin, G. I. Petrov, L. A. Golovan, R. J. Thomas, B. A. Rockwell, and V. V. Yakovlev, *Nat. Commun.* **5**, 4356 (2014).
- ¹²G. I. Petrov, R. Arora, V. V. Yakovlev, X. Wang, A. V. Sokolov, and M. O. Scully, *Proc. Natl. Acad. Sci. U.S.A.* **104**, 7776 (2007).
- ¹³A. Champion and P. Kambhampati, *Chem. Soc. Rev.* **27**, 241 (1998).
- ¹⁴J. N. Bixler, M. T. Cone, B. H. Hokr, J. D. Mason, E. Figueroa, E. S. Fry, V. V. Yakovlev, and M. O. Scully, *Proc. Natl. Acad. Sci. U.S.A.* **111**, 7208 (2014).
- ¹⁵M. T. Cone, J. A. Musser, E. Figueroa, J. D. Mason, and E. S. Fry, *Appl. Opt.* **54**, 334 (2015).
- ¹⁶R. Arora, G. I. Petrov, V. V. Yakovlev, and M. O. Scully, *Anal. Chem.* **86**, 1445 (2014).
- ¹⁷R. Arora, G. I. Petrov, V. V. Yakovlev, and M. O. Scully, *Proc. Natl. Acad. Sci. U.S.A.* **109**, 1151 (2012).
- ¹⁸A. Mahadevan-Jansen, M. F. Mitchell, N. Ramanujam, A. Malpica, S. Thomsen, U. Utzinger, and R. Richards-Kortum, *Photochem. Photobiol.* **68**, 123 (1998).
- ¹⁹S. Duraipandian, W. Zheng, J. Ng, J. J. H. Low, A. Ilancheran, and Z. Huang, *J. Biomed. Opt.* **18**, 067007 (2013).
- ²⁰A. S. Haka, K. E. Shafer-Peltier, M. Fitzmaurice, J. Crowe, R. R. Dasari, and M. S. Feld, *Proc. Natl. Acad. Sci. U.S.A.* **102**, 12371 (2005).
- ²¹S. McAughtrie, K. Faulds, and D. Graham, *J. Photochem. Photobiol., C* **21**, 40 (2014).
- ²²P. Matousek, *Appl. Spectrosc.* **61**, 845 (2007).
- ²³M. J. Pelletier, *Appl. Spectrosc.* **67**, 829 (2013).
- ²⁴R. A. Fisher, *Optical Phase Conjugation* (Academic Press, New York, 1983).
- ²⁵M. Damzen, *Opt. Acta: Int. J. Opt.* **32**, 639 (1985).
- ²⁶I. M. Vellekoop and A. P. Mosk, *Opt. Lett.* **32**, 2309 (2007).
- ²⁷C.-L. Hsieh, Y. Pu, R. Grange, G. Laporte, and D. Psaltis, *Opt. Express* **18**, 20723 (2010).
- ²⁸I. M. Vellekoop, *Opt. Express* **23**, 12189 (2015).
- ²⁹J. Thompson, B. Hokr, and V. Yakovlev, *J. Mod. Opt.* **63**, 80 (2016).
- ³⁰J. V. Thompson, G. A. Throckmorton, B. H. Hokr, and V. V. Yakovlev, *Opt. Lett.* **41**, 1769 (2016).
- ³¹I. M. Vellekoop, E. G. van Putten, A. Lagendijk, and A. P. Mosk, *Opt. Express* **16**, 67 (2008).
- ³²S. M. Popoff, A. Goetschy, S. F. Liew, A. D. Stone, and H. Cao, *Phys. Rev. Lett.* **112**, 133903 (2014); e-print [arXiv:1308.0781](https://arxiv.org/abs/1308.0781).
- ³³R. Sarma, A. Yamilov, S. Petrenko, Y. Bromberg, and H. Cao, *Phys. Rev. Lett.* **117**, 086803 (2016).
- ³⁴G. Ghielmetti and C. M. Aegerter, *Opt. Express* **20**, 3744 (2012).
- ³⁵O. S. Ojambati, J. T. Hosmer-Quint, K.-J. Gorter, A. P. Mosk, and W. L. Vos, *Phys. Rev. A* **94**, 043834 (2016).
- ³⁶O. S. Ojambati, H. Yilmaz, A. Lagendijk, A. P. Mosk, and W. L. Vos, *New J. Phys.* **18**, 043032 (2016).
- ³⁷B. H. Hokr and V. V. Yakovlev, *Opt. Express* **21**, 11757 (2013).
- ³⁸J. N. Bixler, C. A. Winkler, B. H. Hokr, J. D. Mason, and V. V. Yakovlev, *J. Mod. Opt.* **63**, 76–79 (2016).
- ³⁹J. V. Thompson, B. H. Hokr, W. Kim, C. W. Ballmann, B. Applegate, J. Jo, A. Yamilov, H. Cao, M. O. Scully, and V. V. Yakovlev, *Proc. Natl. Acad. Sci. U.S.A.* **114**, 7941 (2017).
- ⁴⁰V. N. Lednev, P. A. Sdvizhenskii, M. Y. Grishin, M. N. Filippov, A. N. Shchegolikhin, and S. M. Pershin, *Opt. Lett.* **42**, 607 (2017).
- ⁴¹P. Matousek, I. P. Clark, E. R. C. Draper, M. D. Morris, A. E. Goodship, N. Everall, M. Towrie, W. F. Finney, and A. W. Parker, *Appl. Spectrosc.* **59**, 393 (2005).
- ⁴²Z. Di, B. H. Hokr, H. Cai, K. Wang, V. V. Yakovlev, A. V. Sokolov, and M. O. Scully, *J. Mod. Opt.* **62**, 97–101 (2015).
- ⁴³B. H. Hokr, J. N. Bixler, G. D. Noojin, R. J. Thomas, B. A. Rockwell, V. V. Yakovlev, and M. O. Scully, *Proc. Natl. Acad. Sci. U.S.A.* **111**, 12320 (2014).
- ⁴⁴W. Becker, *The Bh TCSPC Handbook*, 6th ed. (Becker & Hickl, Berlin, 2014), pp. 1–782.